J. Mech. Phys. Solids, 1968, Vol. 16, pp. 337 to 347. Pergamon Press. Printed in Great Britain.

# PLASTIC STRESS AND STRAIN FIELDS AT A CRACK TIP*

By J. W. Hutchinson
Harvard University, Cambridge, Massachusetts, U.S.A.

(*Received 20th May* 1968)

Summary

Further details of the stress and strain fields associated with the dominant singularity governing the plastic behaviour at a crack tip are presented for conditions of plane stress and plane strain for cracks in both far tensile and far shear fields. Results are obtained for a power hardening material. Limiting cases for non-hardening materials are shown to correspond to certain perfect plasticity solutions.

## 1. Introduction

Most metals, including even the high strength alloys, undergo some plastic deformation in regions of high stress concentration, and fracture precipitated by a crack is nearly always preceded by at least a small amount of plastic deformation at the crack tip. This deformation plays a crucial role in the fracture process which is not yet fully understood. A background discussion of the general problem area has been given by McClintock and Irwin (1965) and Rice (1968). In this paper details of the plastic deformation at a crack tip are presented. This work continues and elaborates on the studies of Cherepanov (1967), Hutchinson (1968), Rice (1967), and Rice and Rosengren (1968). We complete this Introduction with a summary of some of the results contained in these papers.

The discussion which follows is restricted to a small strain formulation of plasticity in which the only nonlinearity introduced into the theory is in the stress–strain relation while the equations of equilibrium and the strain displacement relations are taken to be linear. A deformation theory of plasticity is invoked and a power hardening relation between the plastic strains $\epsilon_{ij}^p$ and the stresses $\sigma_{ij}$ is assumed so that in simple tension $\epsilon^p = \alpha\sigma^n$, and in general

$$\epsilon_{ij}^p = \alpha \tfrac{3}{2} (\sigma_e)^{n-1} s_{ij} \tag{1}$$

where the stress deviator is

$$s_{ij} = \sigma_{ij} - \tfrac{1}{3} \sigma_{pp} \delta_{ij} \tag{2}$$

and

$$\sigma_e^2 = \tfrac{3}{2} s_{ij} s_{ij}. \tag{3}$$

Here $n$ is the power hardening coefficient and $\alpha$ can be regarded as a material constant. Throughout this paper all unbarred stress quantities will have been non-dimensionalized by a tensile yield stress $\bar{\sigma}_Y$ and unbarred strain quantities by the associated tensile yield strain $\bar{\epsilon}_Y$. As implied by (1), plastic deformation

*This work was supported in part by the Advanced Research Projects Agency under Contract SD-88, in part by the National Aeronautics and Space Administration under Grant NsG-559, and by the Division of Engineering and Applied Physics, Harvard University.

is assumed to be independent of the hydrostatic component of the stress and determined by the 'effective stress invariant' $\sigma_e$. The Mises yield condition is simply $\bar{\sigma}_e = \bar{\sigma}_Y$ or $\sigma_e = 1$.

The dominant singularity governing the behaviour at the tip of a line crack as predicted by this theory for either the idealized conditions of *plane stress* or *plane strain* can be obtained in some special cases with the aid of a path independent integral given independently by CHEREPANOV (1967), ESHELBY (1956) and RICE (1967). Application of this integral to the crack problems under discussion reveals that the strain energy density must have an exact $1/r$ variation as the crack tip is approached where $r$ is the distance from the tip. The stress, strain and displacement fields associated with the dominant singularity are

$$\left.\begin{aligned} \sigma_{ij}(r,\theta) &= Kr^{-(1/n+1)}\,\tilde{\sigma}_{ij}(\theta), \\ \sigma_e(r,\theta) &= Kr^{-(1/n+1)}\,\tilde{\sigma}_e(\theta), \\ \tilde{\epsilon}_{ij}^{\,p}(r,\theta) &= \alpha K^n r^{-(n/n+1)}\,\tilde{\epsilon}_{ij}^{\,p}(\theta), \\ u_i(r,\theta) &= \alpha K^n r^{(1/n+1)}\,\tilde{u}_i(\theta), \end{aligned}\right\} \tag{4}$$

where $K$ will be referred to as the amplitude of the singularity*. For small scale yielding, that is when the plastic zone at the tip of the crack is very small compared to the crack length, the amplitude $K$ can also be determined directly by application of the path independent integral.

In the remainder of the paper details of the dominant singularity (4) are presented for a tensile crack under conditions of plane stress and plane strain and for a shear crack under plane strain. The character of these solutions at large values of $n$ (and thus a low strain hardening capacity) is related to certain perfect plasticity solutions.

## 2. PLASTIC DEFORMATION AT THE TIP OF A TENSILE CRACK IN AN INFINITE PLATE UNDER CONDITIONS OF PLANE STRESS

Here it is supposed that the plastic zone at the tip of the crack extends over a distance of more than several sheet thicknesses such that an elastic–plastic theory of plane stress has at least approximate validity everywhere except within a distance of about a thickness or so from the crack tip where three dimensional behaviour is prominent and the assumptions of generalized plane stress break down.

Plots of the $\theta$-variations of the stresses and strains associated with the dominant singularity as given by (4) are given in Fig. 1 for two values of the hardening coefficient $n$. The stress distributions and the calculational details were given by HUTCHINSON (1968). The effective stress invariant for plane stress is

$$\sigma_e^2 = \sigma_r^2 + \sigma_\theta^2 - \sigma_r\,\sigma_\theta + 3\sigma_{r\theta}^2. \tag{5}$$

As seen in Fig. 1 $\tilde{\sigma}_e(\theta)$ has been normalized such that it attains a maximum value of unity. Since the stress distribution is symmetric about a crack subject to a far

*In what follows, the angular coordinate $\theta$ is taken to be zero ahead of the crack and the distance from the tip $r$ has been normalized by the half length of the crack. The amplitude $K$ has been introduced since it is convenient to normalize the $\tilde{\sigma}_{ij}(\theta)$ such that $[\tilde{\sigma}_e(\theta)]_{\max} = 1$.

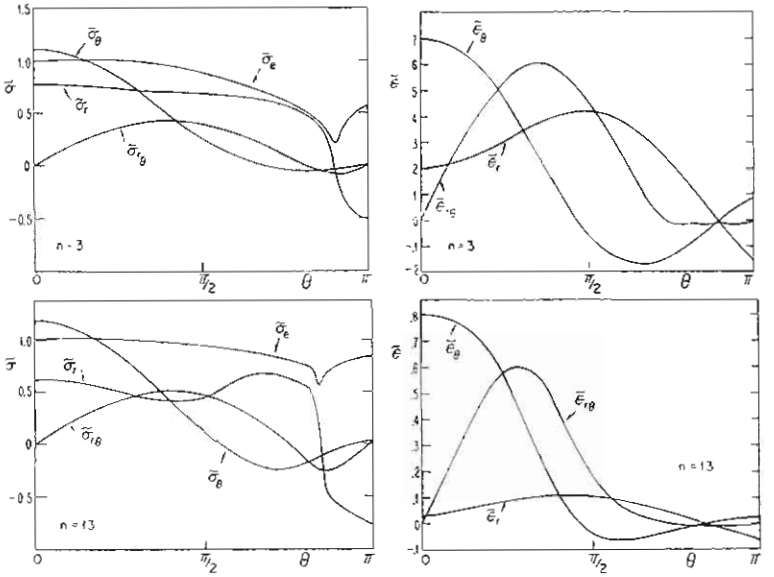


FIG. 1. $\theta$-Variation of stresses and strains at the tip of a tensile crack for plane stress.

tension field, only half the field is displayed. From (1) and (4) the plastic strains are given in terms of the stresses by

$$\begin{aligned} \epsilon_{ij}^{p}(r, \theta) &= \alpha K^{n} r^{-(n/n+1)} \tfrac{3}{2} (\tilde{\sigma}_{e}(\theta))^{n-1} \tilde{s}_{ij}(\theta) \\ &= \alpha K^{n} r^{-(n/n+1)} \tilde{\epsilon}_{ij}^{p}(\theta) \end{aligned} \tag{6}$$

and, thus, by definition of $\tilde{\epsilon}_{ij}^{p}$ :

$$\left.\begin{aligned} \tilde{\epsilon}_{r}^{p}(\theta) &= \tilde{\sigma}_{e}^{n-1} (\tilde{\sigma}_{r} - \tfrac{1}{2} \tilde{\sigma}_{\theta}), \\ \tilde{\epsilon}_{\theta}^{p}(\theta) &= \tilde{\sigma}_{e}^{n-1} (\tilde{\sigma}_{\theta} - \tfrac{1}{2} \tilde{\sigma}_{r}), \\ \tilde{\epsilon}_{r\theta}^{p}(\theta) &= \tfrac{3}{2} \tilde{\sigma}_{e}^{n-1} \tilde{\sigma}_{r\theta}. \\ \tilde{\epsilon}_{z}^{p}(\theta) &= -(\tilde{\epsilon}_{r}^{p} + \tilde{\epsilon}_{\theta}^{p}). \end{aligned}\right\} \tag{7}$$

The amplitude of the dominant singularity for *small scale yielding* is

$$K = \left(\frac{\pi}{\alpha I}\right)^{(1/n+1)} (\sigma^{\infty})^{(2/n+1)} \tag{8}$$

where $\bar{\sigma}^{\infty}$ is the magnitude of the tensile stress far from the crack and $\sigma^{\infty} = \bar{\sigma}^{\infty}/\bar{\sigma}_{Y}$. Numerical values for $I$ for various values of $n$ were given in the previously mentioned reference and are repeated here in Table 1. In the *limit for large* $n$, $I$ appears to approach a constant value ($\approx 2{\cdot}8$) and the strains approach the limiting distribution

$$\tilde{\epsilon}_{ij}^{p}(r, \theta) = \frac{\pi}{I} (\sigma^{\infty})^{2} r^{-1} \tilde{\epsilon}_{ij}^{p}(\theta) \tag{9}$$

while the stresses apparently approach

$$\sigma_{e}(r, \theta) = \tilde{\sigma}_{e}(\theta) = 1 \tag{10}$$

TABLE 1

| $n =$ | | 3 | 5 | 9 | 13 |
|---|---|---|---|---|---|
| Tensile crack Plane stress | I | 3·86 | 3·41 | 3·03 | 2·87 |
| | $\left(\frac{\pi}{I}\right)^{(1/n+1)}$ | 0·949 | 0·987 | 1·004 | 1·006 |
| Tensile crack Plane strain | I | 5·51 | 5·01 | 4·60 | 4·40 |
| | $\left(\frac{\pi}{I}\right)^{(1/n+1)}$ | 0·869 | 0·025 | 0·963 | 0·976 |
| Shear crack Plane strain | I | 0·694 | 0·458 | 0·269 | 0·181 |
| | $\left(\frac{\pi}{I}\right)^{(1/n+1)}$ | 1·46 | 1·38 | 1·29 | 1·23 |

and
$$\sigma_{ij}(r, \theta) = \tilde{\sigma}_{ij}(\theta). \tag{11}$$

In the remainder of this section we explore the relationship between the dominant singularity solutions associated with large values of $n$—thus characterizing a material with a low strain hardening capacity—and predictions based on the theory of perfect plasticity. The perfect plasticity problem will be seen to have a hyperbolic character, while the hardening solutions discussed above are obtained from a system of elliptic equations; even so, a resemblance between the two sets of predictions should be expected if both theories are reasonable models of low strain hardening behaviour.

A general development of the theory of perfect plasticity for plane stress has been given by HILL (1950, p. 300). This theory, with thinning of the plate neglected, is used here to investigate the stress field near a crack in a perfectly plastic thin sheet subject to tension. No attempt has been made to construct the entire solution to this problem. Instead, guided by the character of the dominant singularity of the hardening solution, we construct a stress field centred at the crack tip whose validity is restricted to the immediate vicinity of the tip. The result of this construction is shown in Fig. 2 and is discussed in what follows.

The Mises yield condition for perfect plasticity and plane stress is
$$\sigma_e^2 = \sigma_r^2 + \sigma_\theta^2 - \sigma_r \sigma_\theta + 3\sigma_{r\theta}^2 = 1. \tag{12}$$

On a stress characteristic the normal stress component $\sigma_n$ acting across the characteristic is twice the normal stress component $\sigma_t$ acting along the characteristic. No *continuous* stress field and its associated characteristics could be found which satisfied the stress-free boundary conditions on $\theta = \pm \pi$ and which satisfies the yield condition on the interval $-\pi \leqslant \theta \leqslant \pi$. Indeed, the hardening solutions in Fig. 1, and in particular the low hardening case $n = 13$, strongly hint that a discontinuity in the $\sigma_r$ component of stress should be considered in a perfect plasticity treatment. The possibility of stress discontinuities in perfect plasticity has been discussed by PRAGER (1948) and HILL (1950), and an illustration of a problem in which a stress discontinuity must be introduced has been given by SHIELD (1954).

Continuity of traction across a radial line emanating from the crack tip requires

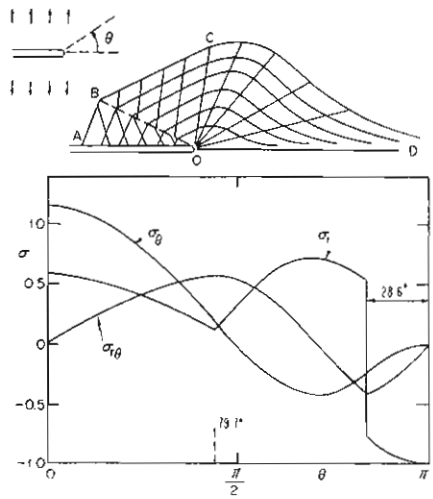


FIG. 2. Stress characteristics and stress distribution at the tip of a tensile crack in a perfectly plastic material for plane stress.

that $\sigma_\theta$ and $\sigma_{r\theta}$ be continuous functions of $\theta$. If the yield eondition is satisfied on both sides of a radial line of discontinuity then the jump in the $\sigma_r$ component of stress can be found from (12) to be

$$\sigma_r^+ - \sigma_r^- = (4 - 3\sigma_\theta^2 - 12\sigma_{r\theta}^2)^{\frac{1}{2}}. \tag{13}$$

Such a discontinuity stems from the idealization inherent to perfect plasticity theory. If elastic strains were taken into account, the radial line across which the jump occurs would actually lie in a narrow elastic region through which the change in $\sigma_r$ as given by (13) takes place.

Condition (13) inferred from the limiting behaviour of the hardening solution enables us to construct a perfect plastic stress field at the tip of the crack. The region AOB in Fig. 2 is subject to uniform stress, $\sigma_{xx} = -1$, $\sigma_{yy} = \sigma_{xy} = 0$, or

$$\sigma_r = -\tfrac{1}{2}(1 + \cos 2\theta), \quad \sigma_\theta = -\tfrac{1}{2}(1 - \cos 2\theta), \quad \sigma_{r\theta} = \tfrac{1}{2}\sin 2\theta. \tag{14}$$

In region BOC the stress is also uniform, but a jump in $\sigma_r$ across the radial line OB is specified according to (13), and thus in BOC

$$\left.\begin{aligned} \sigma_r &= \tfrac{1}{4}(-1 + 3\cos 2\theta_{OB}) + \tfrac{1}{4}(1 + \cos 2\theta_{OB})\cos 2(\theta - \theta_{OB}) \\ &\qquad + \tfrac{1}{2}\sin 2\theta_{OB}\sin 2(\theta - \theta_{OB}), \\ \sigma_\theta &= -\sigma_r + \tfrac{1}{2}(-1 + 3\cos 2\theta_{OB}), \\ \sigma_{r\theta} &= -\tfrac{1}{4}(1 + \cos 2\theta_{OB})\sin 2(\theta - \theta_{OB}) + \tfrac{1}{2}\sin 2\theta_{OB}\cos 2(\theta - \theta_{OB}), \end{aligned}\right\} \tag{15}$$

where $\theta_{OB}$ denotes the angle associated with the line OB to be determined in the subsequent analysis.

If OC is to be a stress characteristic as shown, then $\sigma_r = \frac{1}{2}\sigma_\theta$ on $\theta = \theta_{OC}$ or

$$(-1 + 3\cos 2\theta_{OB}) + 3(1 + \cos 2\theta_{OB})\cos 2(\theta_{OC} - \theta_{OB}) + 6\sin 2\theta_{OB}\sin 2(\theta_{OC} - \theta_{OB}) = 0. \tag{16}$$

In the slip line fan COD the stresses are given by HILL (1952)

$$\sigma_\theta = 2\sigma_r = \frac{2}{\sqrt{3}} \cos\theta; \quad \sigma_{r\theta} = \frac{1}{\sqrt{3}} \sin\theta \tag{17}$$

where the fan has been centred so as to give a symmetric stress field with $\sigma_{r\theta} = 0$ at $\theta = 0$. Continuity of traction across the radial line OC requires continuity of $\sigma_\theta$ and $\sigma_{r\theta}$ at $\theta = \theta_{OC}$ which by (15) and (17) requires

$$\tfrac{1}{4}(-1 + 3\cos 2\theta_{OB}) - \tfrac{1}{4}(1 + \cos 2\theta_{OB})\cos 2(\theta_{OC} - \theta_{OB}) - \tfrac{1}{2}\sin 2\theta_{OB} \sin 2(\theta_{OC} - \theta_{OB}) = \frac{2}{\sqrt{3}} \cos\theta_{OC}. \tag{18}$$

A simple numerical procedure was used to determine $\theta_{OB}$ and $\theta_{OC}$ from (16) and (18) with the result : $\theta_{OB} = 151{\cdot}4^\circ$ and $\theta_{OC} = 79{\cdot}7^\circ$. The stress distribution as given by (14), (15) and (17) are those displayed in Fig. 2.

The distribution of plastic strains at the crack tip according to perfect plasticity theory cannot be obtained by a simple analysis analogous to that for the stresses, although it can easily be shown that there are many possible radial displacement fields consistent with the stress distribution. Certain details of the strain field can be inferred directly from the slip line field of Fig. 2. In particular, the plastic strains can have a $1/r$ singularity—that is, $\tilde{\epsilon}_{ij}^{p}(\theta) \neq 0$ only in the fan region $|\theta| < \theta_{OC}$. Furthermore, in the fan $\sigma_\theta = 2\sigma_r$ and thus $s_r = 0$ and thus the radial component $\tilde{\epsilon}_r^{p}(\theta)$ must vanish for all $\theta$. Both these details as well as the stress distribution itself are clearly reflected in the low strain hardening solution ($n = 13$) in Fig. 1.

GERBERICH (1964) has presented pictures of isochromatic lines in the plastic zones of thin aluminium sheets. These were obtained using a photoelastic coating method and are reproduced in Fig. 3. Along an isochromatic the principal in-plane strain difference, $\epsilon_I - \epsilon_{II}$, is constant. Such isochromatics have been calculated on the basis of the present dominant singularity solution. These are also presented in Fig. 3 for hardening exponents $n = 3$ and $n = 13$ corresponding roughly to the hardening properties of 2040-0 aluminium and 6061-T6 aluminium, respectively. Qualitatively, at least, the agreement is good although the plastic zone of the 6061-T6 specimen is clearly interacting with the boundary.

In our discussions of the perfect plasticity behaviour, we have excluded the possibility of necking ahead of the crack as envisioned in DUGDALE's (1960) model and as treated by HILL (1952) in his analysis of overall yielding of externally notched strips subject to tension. Here, we are concerned with a combination of configuration and material properties such that the plastic zone is relatively small compared to the crack length and such that overall yielding of the specimen does not occur. This is often the situation presented by cracked specimens of structural metals at the point of fracture. Judging from various experimental studies, necking often occurs ahead of a crack in thin sheets of some materials such as mild steel while more diffuse deformation at the crack tip similar to that of the present solution is evident in other materials such as the aluminium specimens investigated by Gerberich.

The dominant singularity of the hardening solution as given by (4) and its amplitude for small scale yielding as given by (8) were obtained on the basis of a deformation theory of plasticity. Deformation theory can be a good representation

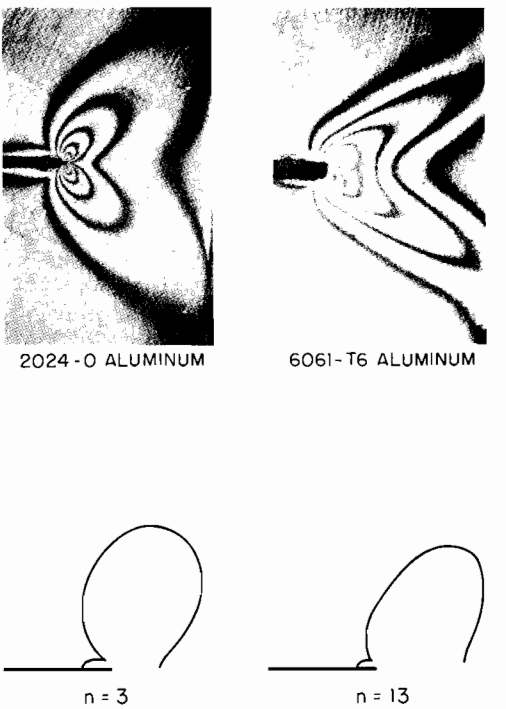


FIG. 3. Isochromatics: upper figures from GERBERICH (1964), lower figures derived from dominant singularity.

of actual plastic deformation only if the loading history at every point is proportional or nearly so as the deformation proceeds (BUDIANSKY 1959). It should be noted that the dominant singularity here is also a solution to the equations of flow theory since the loading is exactly proportional in the regime dominated by the singularity. On the other hand, the amplitude (8) of the singularity would not necessarily follow from a flow theory analysis; and it is difficult to assess the discrepancy between flow and deformation theory analyses in this respect.

## 3. Plastic Deformation at the Tip of a Tensile Crack under Conditions of Plane Strain

The analysis for a crack in a hardening material under conditions of plane strain and subject to a far tension field perpendicular to the crack is analogous to that described in the previous section and has been given by RICE and ROSENGREN (1968) and HUTCHINSON (1968). Stress and strain distributions for this case are shown in Fig. 4. Near the crack tip where the elastic strains can be ignored the Mises yield condition for plane strain is

$$\sigma_e^2 = \tfrac{3}{4}(\sigma_r - \sigma_\theta)^2 + 3\sigma_{r\theta}^2. \tag{19}$$

The plastic strains are again given by (4) where now

$$\tilde{\epsilon}_r^p = -\tilde{\epsilon}_\theta^p = \tfrac{3}{4}\tilde{\sigma}_e^{n-1}(\tilde{\sigma}_r - \tilde{\sigma}_\theta); \quad \tilde{\epsilon}_{r\theta}^p = \tfrac{3}{2}\tilde{\sigma}_e^{n-1}\tilde{\sigma}_{r\theta}. \tag{20}$$

For small scale yielding the amplitude $K$ of the dominant singularity is

$$K = \left[\frac{\pi(1-\nu^2)}{\alpha I}\right]^{(1/n+1)} [\sigma^\infty]^{(2/n+1)} \tag{21}$$

where $\nu$ is Poisson's Ratio. The limiting form of the solution for vanishing hardening capacity (i.e., $n \to \infty$) is that given by (9) [except for a factor $(1-\nu^2)$], (10) and (11)—and the limit value for $I$ is about 4.3

The stress distribution and slip line field at the tip of a crack as predicted by the well known perfect plasticity solution of PRANDTL (1920) and HILL (1951) is given in Fig. 5. As noted by RICE and ROSENGREN (1968), the stress distribution of the hardening solution for large $n$ closely approximates that given by the perfect plasticity solution as can be seen from a comparison of the $n = 13$ solution of Fig. 4 with the plots of Fig. 5 and the $n \to \infty$ limit clearly appears to be the perfect plasticity solution.

The strain distribution at the crack tip according to perfect plasticity theory has not been found, but here again the plastic strains will be largest (i.e., a non-vanishing $1/r$ singularity) within the fans on the top and bottom of the crack where the only nonzero component will be $\epsilon_{r\theta}^p$. These features are reflected by the low strain hardening solution of Fig. 4. In a related study NEIMARK (1968) introduced strain hardening in his analysis of a doubly V-notched bar and with the aid of an extremum principle for strain hardening materials was able to approximate the displacement and strain fields at the notch.

Plane strain conditions at the tip of a crack result in a significantly higher tensile stress ahead of the crack than is found under conditions of plane stress. Using the stress ahead of the crack found from the Prandtl–Hill solution and that for the tensile crack under plane stress (17), the ratio is found to be

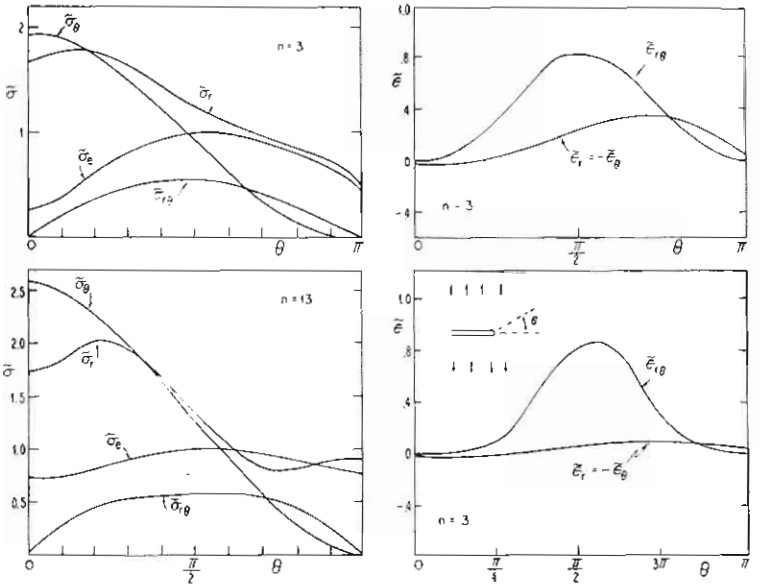


FIG. 4. $\theta$-Variations of stress and strains at the tip of a tensile crack for plane strain.

$$\frac{\sigma_\theta\,(\theta = 0)_{\text{plane strain}}}{\sigma_\theta\,(\theta = 0)_{\text{plane stress}}} = 1 + \frac{\pi}{2}\,. \tag{22}$$

This value is the $n \to \infty$ limit for the ratio of the two amplitudes of the tensile stress singularity ahead of the crack for the hardening solutions given by HUTCHINSON (1968).

## 4. PLASTIC DEFORMATION AT THE TIP OF A CRACK IN A SHEAR FIELD UNDER CONDITIONS OF PLANE STRAIN

Figure 6 displays plots of the $\theta$-variations of the stresses and strains of the dominant singularity at the tip of a crack under conditions of plane strain which is subject to pure shear parallel to the crack far from it. These results were obtained using the same procedure as has been applied to the crack in a tension field. Equations (1)–(4), (6), (19) and (20) apply here as well. In this case the amplitude of the singularity when the plastic zone is very small is

$$K = \left(\frac{\pi\,(1 - \nu^2)}{\alpha I}\right)^{(1/n+1)} \left[\sigma^\infty{}_{xy}\right]^{(2/n+1)} \tag{23}$$

where the crack is taken to be aligned with the $x$ axis and where $\bar{\sigma}^\infty{}_{xy}$ is the non-zero component of stress far from the crack and $\sigma^\infty{}_{xy} = \bar{\sigma}^\infty{}_{xy}/\bar{\sigma}_Y$. Numerical values for $I$ and $(\pi/I)^{(1/n+1)}$ are given in Table 1.

Stresses and slip lines associated with a local radial field centred at the crack tip are shown in Fig. 7. These have been determined on the basis of the well known plane strain equations of perfect plasticity. Here again, it has not been possible to determine the strain distribution at the crack tip other than to note that a

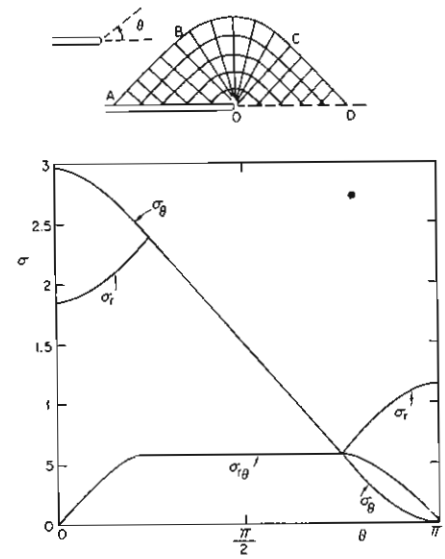


FIG. 5. Stress characteristics and stress distribution at tip of a tensile crack in a perfectly plastic material for plane strain.

$1/r$ singularity in strains can occur only in the fan regions and that, since the slip lines do not extend, $\tilde{\epsilon}_r$ and $\tilde{\epsilon}_\theta$ are zero in the fans. These details and the near coincidence of the stresses of the perfect plasticity field and those of the ($n = 13$) solution of Fig. 6 strongly suggest that the limit stress field of the dominant singularity of the hardening solution is the perfect plasticity solution given in Fig. 7.

The stress distribution and slip line field at the crack tip have simple forms.

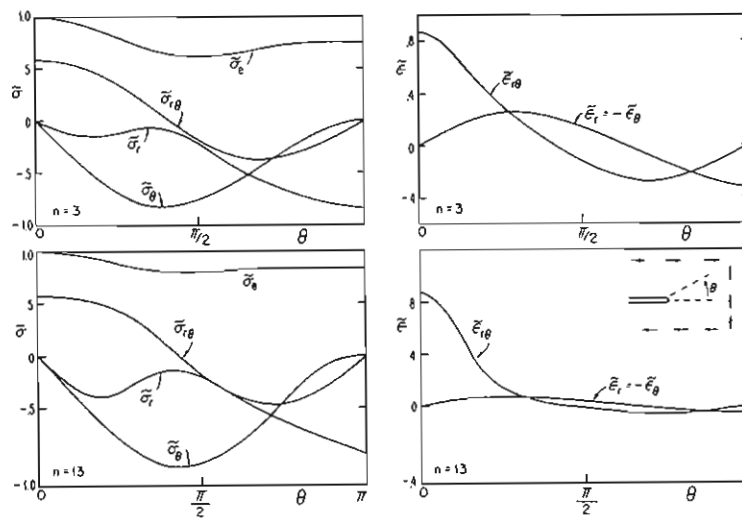


FIG. 6. $\theta$-Variations of stresses and strains at the tip of a shear crack for plane strain.

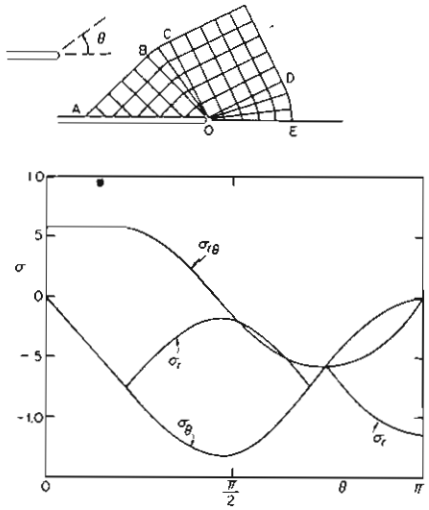


FIG. 7. Characteristics and stress distribution at the tip of a shear crack for plane strain.

In the region AOB the stress state is homogeneous with $\sigma_x = -2/\sqrt{3}$ and $\sigma_y = \sigma_{xy} = 0$ or

$$\sigma_r = -\frac{1}{\sqrt{3}}(1 + \cos 2\theta); \quad \sigma_\theta = -\frac{1}{\sqrt{3}}(1 - \cos 2\theta); \quad \sigma_{r\theta} = \frac{1}{\sqrt{3}}\sin 2\theta. \quad (24)$$

In the fan BOC

$$\sigma_r = \sigma_\theta = -\frac{1}{\sqrt{3}}\left[1 + 2\left(\frac{3\pi}{4} - \theta\right)\right]; \quad \sigma_{r\theta} = -\frac{1}{\sqrt{3}}. \quad (25)$$

The stress state in COD is uniform and on $\theta = \theta_{OC}$ takes on the values

$$\sigma_r = \sigma_\theta = -\frac{1}{\sqrt{3}}\left[1 + 2\left(\frac{3\pi}{4} - \theta_{OC}\right)\right]; \quad \sigma_{r\theta} = -\frac{1}{\sqrt{3}}. \quad (26)$$

In the fan ahead of the crack

$$\sigma_r = \sigma_\theta = -\frac{2}{\sqrt{3}}\theta; \quad \sigma_{r\theta} = \frac{1}{\sqrt{3}} \quad (27)$$

and continuity of traction across OD requires $\theta_{OC} = \frac{5\pi}{8} + \frac{1}{4}$.

Note that the maximum tensile stress which develops at the tip of a perfectly plastic tensile crack under plane strain conditions is substantially larger than predicted for the shear crack. At the same time an examination of the numerical values for the strains reveals that the plastic strains at the tip of a shear crack appear to be almost an order of magnitude larger than those at a tensile crack at a given distance from the crack tip and at a comparable level of applied stress.

## REFERENCES

BUDIANSKY, B. 1959 *Trans. Am. Soc. Mech. Engrs* **81E**, 259.

| | | |
|---|---|---|
| CHEREPANOV, G. P. | 1967 | *J. Appl. Math. and Mech.* (PMM) (Translated from the Russian), **31**, 503. |
| DUGDALE, D. | 1960 | *J. Mech. Phys. Solids* **8**, 100. |
| ESHELBY, J. D. | 1956 | *Solid State Physics*, Vol. 3, p. 79. Edited by SEITZ, F. and TURNBULL, D. (Academic Press, N.Y.). |
| GERBERICH, W. W. | 1964 | *Exp. Mech.* **4**, 335. |
| HILL, R. | 1950 | *The Mathematical Theory of Plasticity* (Clarendon Press, Oxford). |
| | 1951 | *Phil. Mag.* **42**, 868. |
| | 1952 | *J. Mech. Phys. Solids* **1**, 19. |
| HUTCHINSON, J. W. | 1968 | *J. Mech. Phys. Solids* **16**, 13. |
| McCLINTOCK, F. A. and IRWIN, G. R. | 1965 | *Am. Soc. Test. Mater.* Special Publication 381. |
| NEIMARK, J. E. | 1968 | *J. Appl. Mech.* **35**, 111. |
| PRAGER W. | 1948 | *Courant Anniversary Volume*, p. 289 (Interscience Publishers, N.Y.). |
| PRANDTL, L. | 1920 | *Nachr. Ges. Wiss., Göttingen*, 74. |
| RICE, J. R. | 1967 | Brown University Engineering Report, No. E39. |
| | 1968 | Am. Soc. Test. Mater. Special Technical Publication 415. |
| RICE, J. R. and ROSENGREN, G. | 1968 | *J. Mech. Phys. Solids* **16**, 1. |
| SHIELD, R. T. | 1954 | *J. Math. and Phys.* **33**, 144. |